Biosensors and Bioelectronics 85 (2016) 272–279

Contents lists available at ScienceDirect

Biosensors and Bioelectronics

journal homepage: www.elsevier.com/locate/bios

Hepatitis B plasmonic biosensor for the analysis of clinical serum samples

Tomáš Riedel [a,*], František Surman [a], Simone Hageneder [b], Ognen Pop-Georgievski [a], Christa Noehammer [c], Manuela Hofner [c], Eduard Brynda [a], Cesar Rodriguez-Emmenegger [a,d,**], Jakub Dostálek [b,***]

[a] Institute of Macromolecular Chemistry AS CR v.v.i., Heyrovsky Sq. 2, 162 06 Prague 6, Czech Republic
[b] Biosensor Technologies, AIT-Austrian Institute of Technology GmbH, Muthgasse 11, 1190 Vienna, Austria
[c] Molecular Diagnostics, Health and Environment Dpt., AIT-Austrian Institute of Technology GmbH, Muthgasse 11, 1190 Vienna, Austria
[d] DWI – Leibniz Institute for Interactive Materials and Institute of Technical and Macromolecular Chemistry, RWTH Aachen University, Forckenbeckstraße 50, 52074 Aachen, Germany

ARTICLE INFO

Article history:
Received 18 March 2016
Received in revised form
4 May 2016
Accepted 5 May 2016
Available online 6 May 2016

Keywords:
Surface plasmon resonance
Biosensors
Polymer brushes
Antifouling
Hepatitis B
Blood serum

ABSTRACT

A plasmonic biosensor for rapid detection of protein biomarkers in complex media is reported. Clinical serum samples were analyzed by using a novel biointerface architecture based on poly[(*N*-(2-hydroxypropyl) methacrylamide)-*co*-(carboxybetaine methacrylamide)] brushes functionalized with bioreceptors. This biointerface provided an excellent resistance to fouling even after the functionalization and allowed for the first time the direct detection of antibodies against hepatitis B surface antigen (anti-HBs) in clinical serum samples using surface plasmon resonance (SPR). The fabricated SPR biosensor allowed discrimination of anti-HBs positive and negative clinical samples in 10 min. Results are validated by enzyme-linked immunoassays of the sera in a certified laboratory. The sensor could be regenerated by simple treatment with glycine buffer.

1. Introduction

As the infection by hepatitis B virus (HBV) can cause potentially life-threatening diseases such as chronic hepatitis, cirrhosis, or even liver cancer, it represents one of the major global health threats. Almost one third of the world population is infected by the HBV, from which over 250 million people become chronically infected, and more than 780 thousand people die every year due to complications related to hepatitis B (Lozano et al., 2012). The rate of prevalence reaches up to 10% in developing countries in Africa and East Asia (Hollinger and Liang, 2001) and even up to 20% in the Asia-Pacific region (Lesmana et al., 2006). The prevalence is much lower in western countries such as Germany, under 1%, which represents a total HBV-related cost exceeding 600 million EUR per year (Harbarth et al., 2000). HBV is easily transmitted by the exposure to infected blood or body fluids. Infection of humans by HBV is accompanied with the production of antibodies against the antigens presented on the HBV surface.

The infection and further spreading of the virus can be efficiently prevented by vaccination with the purified and recombinant surface antigen of the hepatitis B virus (HBsAg). However, the duration of the protection varies and regular check of the antibody titer is recommended, especially in the groups with elevated risk such as hospital staff (Gitlin, 1997; Poorolajal et al., 2010). Currently, the most commonly used technique for serological diagnostic is ELISA, however its use is restricted to centralized laboratories as it requires highly trained personnel and relies on multiple-step procedures. Thus, preventing the use of ELISA for point-of-care diagnostics (Tighe et al., 2015).

In order to perform diagnostic assays outside specialized laboratories and carry out the analysis closer to patients, we witnessed the development of biosensor technologies for point-of-care analysis of human plasma/serum and other accessible bodily fluids (Wang et al., 2010; Yao and Fu, 2014). However, none of these examples showed the detection in real clinical samples nor at biologically relevant concentrations of the markers. Therefore, it

* Corresponding author at: Institute of Macromolecular Chemistry AS CR v.v.i., Heyrovsky Sq. 2, 162 06 Prague 6, Czech Republic.
** Corresponding author at; DWI – Leibniz Institute for Interactive Materials and Institute of Technical and Macromolecular Chemistry, RWTH Aachen University, Forckenbeckstraße 50, 52074 Aachen, Germany.
*** Corresponding author at: Biosensor Technologies, AIT-Austrian Institute of Technology GmbH, Muthgasse 11, 1190 Vienna, Austria
E-mail addresses: riedel@imc.cas.cz (T. Riedel), rodriguez@dwi.rwth-aachen.de (C. Rodriguez-Emmenegger), jakub.dostalek@ait.ac.at (J. Dostálek).

http://dx.doi.org/10.1016/j.bios.2016.05.014
0956-5663/

is of high interest to develop detection techniques that provide fast response, high sensitivity, and possibilities for the miniaturization required for personalized medicine. Optical affinity biosensors represent a promising technology allowing fast high-throughput and in-real time detection (Homola, 2008; Stewart et al., 2008). Numerous SPR based biosensors were reported for the rapid detection of the anti-HBs or even the HBV viral DNA in the last years (Choi et al., 2014; Chuang et al., 2012, 2005; Hwang et al., 2005; Lu et al., 2013; Uzun et al., 2009; Wang et al., 2010; Zheng et al., 2010). These works demonstrate the detection in buffer, spiked serum, or detection of viral DNA after its separation and amplification. It is noteworthy that none of these examples achieved the detection of biologically relevant concentrations in clinical samples. Presumably, the high fouling observed in the clinical samples hampers the direct detection. Therefore, the analysis of complex matrices requires advanced biointerface architectures that are sufficiently resistant to fouling which impedes the sensor specificity by unspecific adsorption.

Arguably, protein fouling is the most critical technical challenge preventing plasmonic (and other affinity) biosensors reaching clinical practice (Blaszykowski et al., 2015). This effect leads to unspecific adsorption that blocks the sensor surface and hinders its ability to discriminate the specific binding of target analyte. To prevent fouling self-assembled monolayers (SAM) of alkanethiols terminated with variable functional units are often used (Blaszykowski et al., 2015). However, they do not provide sufficient resistance when challenged with complex biological media such as serum (Chung et al., 2005; Herrwerth et al., 2003; Riedel et al., 2014, 2013; Rodriguez Emmenegger et al., 2009).

Polymer brushes prepared by surface-initiated radical polymerization, have been shown to efficiently reduce or even completely suppress the fouling from complex biological media (Blaszykowski et al., 2012; Cho et al., 2014; Rodriguez-Emmenegger et al., 2012b). Poly(carboxybetaine acrylamide) (poly (CBAA)) and poly[*N*-(2-hydroxypropyl) methacrylamide] (poly (HPMA)) brushes were demonstrated to completely eliminate fouling from blood plasma, the most widely used bodily fluid for biosensing (Jiang and Cao, 2010; Rodriguez-Emmenegger et al., 2011; Yang et al., 2009). Moreover, poly(HPMA) brushes resist fouling from complex biological media, such as human blood plasma and serum, calf serum, fetal serum, urine, cerebrospinal fluid and saliva (Rodriguez-Emmenegger et al., 2012b). In addition, the polymer brushes resisted fouling of whole blood and its components, prevent adhesion of cells (rat embryonic fibroblasts), reduce bacteria adhesion and biofilm formation, and they even display non-thrombogenic surface properties (de Los Santos Pereira et al., 2016; Pop-Georgievski et al., 2013; Rodriguez-Emmenegger et al., 2015, 2013; Surman et al., 2015). The resistance of carboxybetaines polymer layers is ascribed to electrostatically induced hydration layer (Jiang and Cao, 2010) while the resistance of poly(HPMA) brushes is still under scrutiny.

The preparation of affinity biosensors not only requires excellent resistance to fouling as well as the presence of functional groups exploitable for immobilization of bioreceptors. The facile activation of all functional groups along the polymer chain led to several affinity biosensors (Brault et al., 2013; Mahmud et al., 2011; Vaisocherová et al., 2008). However, it has been shown that the activation and biofunctionalization lead to irreversible changes in fouling (Vaisocherová et al., 2014). While this problem is usually neglected, careful evaluation of the presented published data showed always reference-compensated signals as a result of the increment in fouling (Vaisocherová et al., 2008). A feasible way to circumvent this problem is to activate and functionalize only a small fraction of the functional groups. For instance, two monomers with distinct side groups can be copolymerized and by using an orthogonal reaction which activates the sides groups of only one of the monomers, it is possible to create only minimal changes in the brush preserving the non-fouling properties. Building on this concept we developed a biosensing platform able to detect anti-HBs antibodies. The surface was prepared by the statistic copolymerization of two non-fouling monomers, HPMA and CBMAA, by surface initiated atom transfer radical polymerization (SI-ATRP). Upon activation HBsAg antigen was immobilized on the brushes with no increase in the fouling. This was exploited to fabricate a new plasmonic biosensor for the analysis of anti-HBs in real clinical serum samples using SPR. It takes advantage of a novel antifouling poly[(*N*-(2-hydroxypropyl) methacrylamide)-*co*-(carboxybetaine methacrylamide)] (poly (HPMA-*co*-CBMAA)) brush that retains its properties even after the immobilization of large surface mass density of ligands.

2. Materials and methods

2.1. Materials

All materials were used as purchased otherwise stated. A detailed list can be found in the SI.

2.2. Biological samples

Serum samples were collected from eight healthy donors who were either vaccinated or not-vaccinated against Hepatitis B. Blood samples were incubated in Vacuette 9 mL Z Serum Clot Activator (Greiner Bio One, Frickenhausen, Germany) for 30 min followed by centrifugation for 10 min at 1800 *g* at room temperature. Aliquots were stored at −80 °C before analysis. Serum samples were tested for the presence of anti-HBs antibodies in CE certified laboratory Labors at in Vienna (Austria) by using regular enzyme-linked immunoassays (ELISA).

2.3. Synthesis of poly(HPMA-co-CBMAA) brushes via SI-ATRP

Gold-coated glass slides (SPR chips) were first incubated with ω-mercaptoundecyl bromoisobutyrate, an ATRP initiator, as described previously (Rodriguez Emmenegger et al., 2009). The polymerization of poly(HPMA-*co*-CBMAA) brushes is schematically showed in Fig. 1. Firstly, 7 mL of methanol was degassed via six freeze-pump-thaw cycles and subsequently transferred under argon atmosphere to a Schlenk tube containing CuCl (35 mg, 354 μmol), $CuCl_2$ (10.5 mg, 78 μmol) and Me_4Cyclam (121 mg, 472 μmol). The catalyst mixture was stirred until all solids were dissolved. In a second Schlenk tube, HPMA (2.4 g, 16.6 mmol) and CBMAA (0.7 g, 2.9 mmol) were dissolved in 12 mL of water previously degassed via six freeze-pump-thaw cycles and 5 mL of deoxygenated methanol and kept at 0 °C. After complete dissolution, the blue catalyst solution was transferred to the monomer solution using a gastight syringe. Subsequently, the homogenized polymerization mixture was cannulated into the reactor containing the substrates coated with the initiator SAM. The polymerization was carried out at 30 °C for 2 h. The samples were taken out of the reactor, washed thoroughly with water and stored in water until the use.

2.4. Characterization of poly(HPMA-co-CBMAA) brushes

X-ray photoelectron spectroscopy (XPS) measurements were carried out with a K-Alpha+ spectrometer (ThermoFisher Scientific). Data acquisition and processing were performed using Thermo Advantage software. All spectra were referenced to the C1s peak of hydrocarbons at 285.0 eV BE controlled by means of the well-known photoelectron peaks of PET and metallic Cu, Ag,

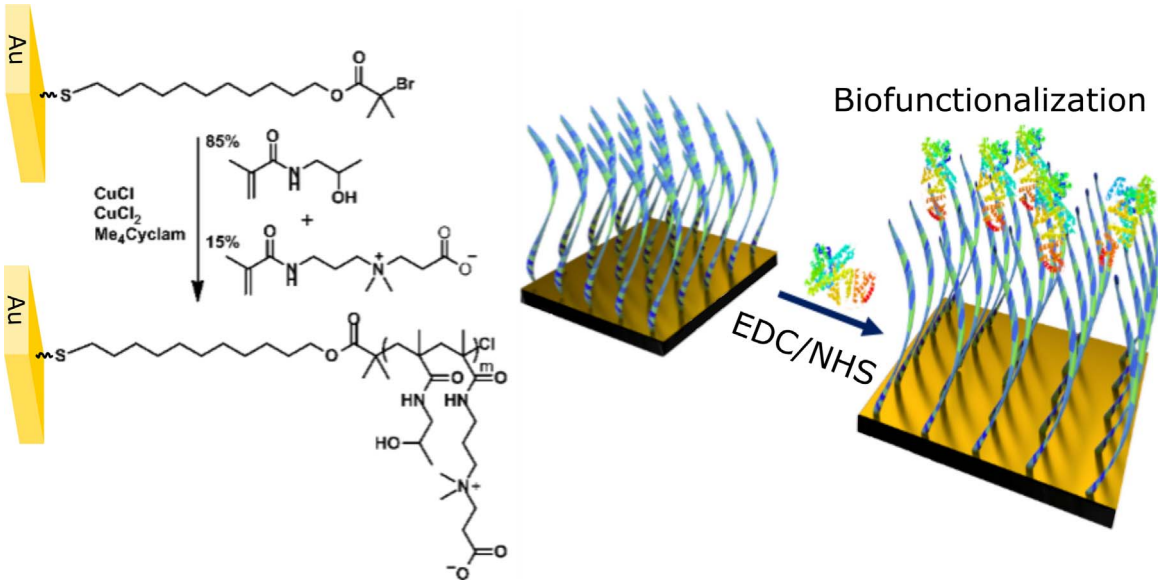

Fig. 1. Synthesis and chemical structure of the poly(HPMA-*co*-CBMAA) polymer brush (left) and schematics of gold surface with tethered brush that is post-modified with protein ligand (right).

and Au. For details see SI.

Fourier transform infrared grazing angle specular reflectance spectroscopy (FTIR-GASR) was carried out using a Nicolet Nexus 870 with a SAGA attachment. The spectra were acquired with 256 scans at a resolution of 2 cm^{-1} and processed with OMNIC software. The spectrometer was purged continuously with dry air.

Ellipsometric data were acquired using a spectroscopic ellipsometer M2000 (J.A. Woollam Co., USA) operated in rotating compensator mode. All measurements were performed in the wavelength range of 350–1000 nm with a Xe arc lamp light source and angle of incidence of 60°. For the measurements in water, a liquid cell with a volume of V=0.7 mL was used. The obtained data were analyzed with the CompleteEASE software. For more details refer to the SI.

The wettability of surfaces was examined by dynamic sessile water drop method using a DataPhysics OCA 20 contact angle system. A 5 μL water drop was placed on the surface, and advancing and receding contact angles were determined while the volume of the drop was increased up to 15 μL and decreased at flow rate of 0.5 μL s^{-1}. The data were evaluated using the Young–Laplace method. Reported values were averaged over at least three measurements recorded at different positions on each substrate.

Atomic force microscopy (AFM) was employed to investigate the morphology of the brushes by using a Multimode Atomic Force Microscope NanoScope IIIa (Digital Instruments). Topographical scans in tapping mode were measured in air using OTESPA tips. Areas of 5×5 μm^2 were scanned at a rate of 1 Hz. The scans were analyzed using Gwyddion software.

2.5. Optical setup of plasmonic biosensors

SPR-based detection was performed by using an instrument with wavelength interrogation of SPR which was developed at the Institute of Photonics and Electronic of the Academy of Sciences of the Czech Republic (Homola et al., 2002) (Fig. 2a). The angle of incidence of the polychromatic beam θ was adjusted in order to tune the SPR wavelength close to λ_{SPR}=750 nm. The binding induced variations in λ_{SPR} were tracked in time by using dedicated

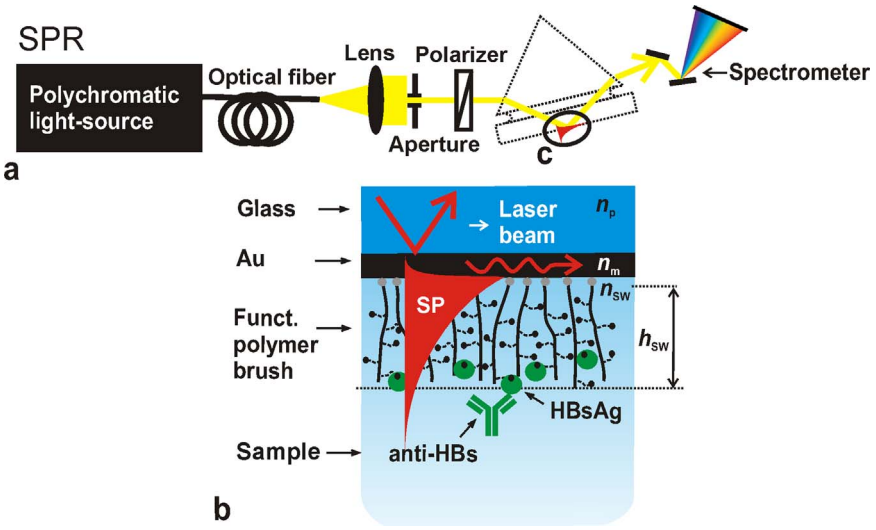

Fig. 2. Schematic diagram of the surface plasmon resonance setup (a). Sensor chip with poly(HPMA-*co*-CBMAA) brush functioning as a binding matrix for direct detection of anti-HBs target analyte (b).

software. The sensor allowed for the monitoring of refractive index changes on the sensor surface with the resolution of 3×10^{-7} refractive index units (RIU). A flow-cell with four chambers (each with a volume of 1 μL) was clamped against the sensor surface and analyzed liquid samples were flowed by using a peristaltic pump with a flow rate of 15 μL min^{-1}. The limit of detection of the SPR is 0.3 ng cm^{-2} (de los Santos Pereira et al., 2014). All measurements were carried out at $T=25$ °C.

2.6. Determination of fouling from blood serum on poly(HPMA-co-CBMAA) brushes

The irreversible adsorption (fouling) of biological components from blood serum on poly(HPMA-*co*-CBMAA) brushes was quantitatively determined by SPR. After establishing a stable baseline of SPR sensor signal λ_{SPR} in PBS buffer (pH 7.4), undiluted human blood serum from healthy individuals were flowed over the surface of the brushes for 10 min, followed by washing with PBS. The fouling was estimated by the difference in sensor baselines before and after contact with serum.

2.7. Immobilization of HBsAg on poly(HPMA-co-CBMAA) brush

The antigen HBsAg was tethered to carboxylic groups available in the brushes previously activated using the amine coupling reaction as indicated in Fig. 1. Firstly, the brush surface was contacted with SA buffer pH 5. Subsequently, the surface was reacted with a freshly prepared solution 1:1 v/v of EDC (0.4 M) and NHS (0.1 M) for 10 min to form active succinimidyl esters. Then the surface was subsequently rinsed with SA and HEPES buffers for one minute each and the antigen, HBsAg (25 μg mL^{-1} in HEPES buffer), was flowed over surface for up to 25 min. Finally, the unreacted active ester groups were let to hydrolyze by flowing PBS for 90 min.

2.8. Detection assay

The prepared surfaces comprise brushes of poly(HPMA-*co*-CBMAA) on which antigen HBsAg was covalently immobilized. Blood serum samples with the volume of 15 μL were diluted in PBS at the volumetric ratio 1:10. A baseline in sensor response was established upon a flow of PBS. Afterwards, the analyzed sample was injected to the sensor for 10 min followed by 5 min rinsing by PBS buffer. The affinity binding of target anti-HBs analyte to HBsAg was directly observed by measuring the sensor signal λ_{SPR}. The sensor response was defined as a difference in the SPR wavelength $\Delta\lambda_{SPR}$ before the sample injection and after the 5 min rinsing with PBS. All measurements were carried out at least in triplicate.

3. Results and discussion

Statistical copolymer brushes of HPMA and CBMAA were prepared for the first time. While both monomers have been used in the past to prepare the only two truly non-fouling surface modifications the combination of both polymers have never been presented. The brushes were biofunctionalized with HBsAg by an orthogonal activation of carboxylic groups at the surface to prepare biosensors to detect markers of hepatitis B in blood serum.

3.1. Physicochemical characterization of poly(HPMA-co-CBMAA) brush

Poly(HPMA-*co*-CBMAA) copolymer brush was successfully grown from a densely packed SAM of ω-mercaptoundecyl bromoisobutyrate on Au via SI-ATRP. Such polymerization is known to be not well controlled which is a typical feature for the ATRP of methacrylamide monomers. However, the combination of the previously optimized conditions (Rodriguez-Emmenegger et al., 2011, 2012a) allowed to synthesize poly(HPMA-*co*-CBMAA) brush with a reproducible thickness.

The grafting of the polymer brushes by surface-initiated ATRP is accompanied by pronounced changes in the C 1s region of the XPS spectrum compared to the SAM of initiator. The high resolution C1s and N1s spectra of the poly(HPMA-*co*-CBMAA) brushes (Fig. 3a and b and Supporting Information) shows the characteristic contributions observed in the XPS spectra of both homopolymer brushes (poly(HPMA) and poly(CBMAA)). The core level C 1s spectrum is characterized by a C–C, C–H contribution at 285.0 eV which is accompanied by a contribution at 285.6 ± 0.1 eV arising from the secondary chemical shift, *i.e.* the effect of the ester group on the tertiary carbon atom in the C*–C(=O)–O–R structure (Fig. 3a). The peak at 286.2 ± 0.2 eV stems from the C–N moiety and is well resolved from the C–O–H contribution at 286.9 ± 0.1 eV. The amide group C(=O)–NH is present at 288.0 ± 0.1 eV and is well resolved from the carboxyl (O–C=O) peak at 288.6 ± 0.3 eV. The presence of both HPMA and CBMAA monomer units in the poly(HPMA-*co*-CBMAA) brushes is also corroborated in the high resolution N 1s spectrum presented in Fig. 3b. The N 1s spectrum exhibits a peak at 400.0 eV stemming from amides bond of HPMA and CBMAA and an additional contribution at 402.9 eV which is assigned to the positively charged quaternary ammonium forming the zwitterion from CBMAA (N 1s spectra of homopolymers is presented in the SI). The fraction of CBMAA in the copolymerized brushes was calculated from the N 1s spectrum as 12%. This value is close to the ratio in the feed as expected from the similar polymerization rate of both monomers. The FTIR GASR spectrum of poly(HPMA-*co*-CBMAA) brushes (Fig. 3c) exhibits the amide I and II bands at 1527 and 1653 cm^{-1}. A band at 1376 cm^{-1} and a shoulder band at 1610 cm^{-1} correspond to the symmetric and asymmetric stretching modes of COO^- stemming from CBMAA.

The wettability was evaluated by advancing and receding water contact angles. The novel copolymer based on poly(HPMA-*co*-CBMAA) displayed wettability of $\theta_{adv}=34 \pm 0.5°$; $\theta_{rec}=15.3 \pm 3.3°$. Compared to the polymer brushes based on poly(HPMA) ($\theta_{adv}=40°$; $\theta_{rec}=21°$) and poly(CBAA) ($\theta_{adv}=23°$; $\theta_{rec}=8°$), the new copolymer brush displayed both advancing and receding contact angle in between the values measured for the homopolymers (Jiang and Cao, 2010; Rodriguez-Emmenegger et al., 2011). The hydration of the poly(HPMA-*co*-CBMAA) brush in water was obtained from its swelling ratio in water of SR=179%, determined from the ellipsometric dry and swollen film thickness ($h_{dry}=29.2 \pm 2.3$ nm and $h_{sw}=81.5 \pm 1.7$ nm) using Eq. (1). It is worth of noting that the swelling ratio was similar to that observed for homopolymer brushes composed of only poly(HPMA) (SR=176%) and poly(CBAA) (SR=190%). The volume fraction of water in the swollen copolymer brush was obtained from the brush thickness in dry and in swollen state using Eq. (2) which yields $f_h=0.64 \pm 0.04$. This value is in good agreement with the volume fraction of water calculated applying the Lorentz-Lorenz effective medium theory: $f_{L\text{-}L\ EMA}=0.69 \pm 0.05$, obtained using Eq. (3) employing the refractive indices of swollen polymer brush ($n_{sw}=1.3866$), dry polymer ($n_{dry}=1.4956$) obtained from the ellipsometric measurements and water ($n_{H2O}=1.3389$ from the literature) at $\lambda=500$ nm.

$$SR = \frac{h_{sw} - h_{dry}}{h_{dry}}. \quad (1)$$

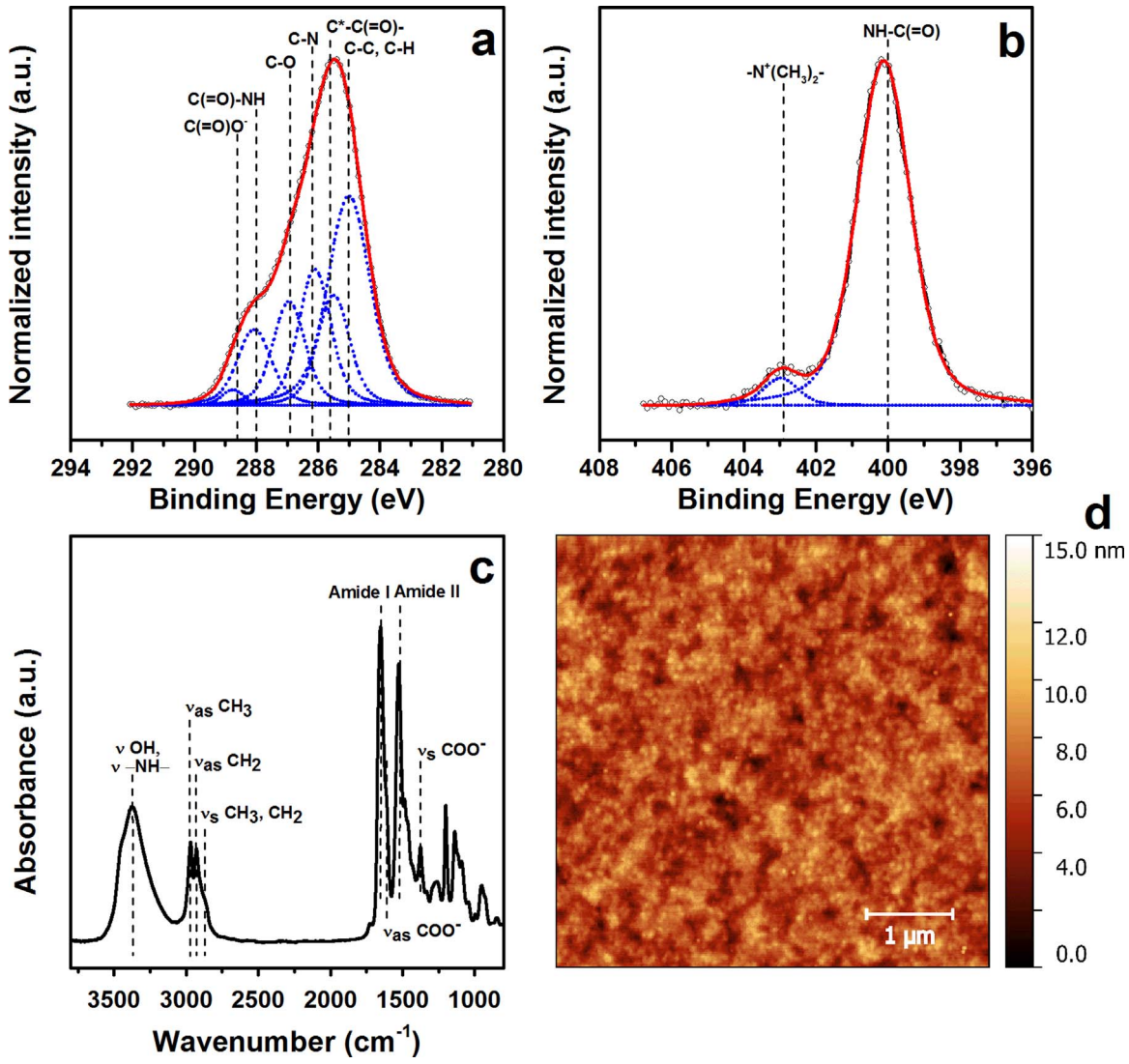

Fig. 3. Characterization of the poly(HPMA-*co*-CBMAA) copolymer brush. (a) High resolution of C 1s and (b) N 1s XPS spectra, (c) FTIR GASR spectrum, and (d) representative AFM topography image (scale bar is 1 μm).

$$f_h = \frac{h_{sw} - h_{dry}}{h_{sw}}, \tag{2}$$

$$f_{L-L\,EMA} = \frac{\frac{n_{sw}^2 - n_{dry}^2}{n_{sw}^2 + 2n_{dry}^2}}{\frac{n_{H_2O}^2 - n_{dry}^2}{n_{H_2O}^2 + 2n_{dry}^2}}, \tag{3}$$

The morphology of poly(HPMA-*co*-CBMAA) polymer brush was examined by AFM in the swollen state (Fig. 3d). The surface of the brush was smooth, without uncovered areas and displayed a low (root means square) roughness of Rq = 1.4 ± 0.08 nm. Homogenous polymer layer without visible pinholes is generally signature of well controlled polymerization and a prerequisite good resistance to protein fouling (Shi et al., 2012).

3.2. Immobilization of HBsAg on non-fouling brushes

The activation and biofunctionalization of poly(HPMA-*co*-CBMAA) brush were carried out *in situ* and monitored by the SPR, as depicted in Fig. 4a. The carboxylic groups present in CBMAA monomeric units were activated by 10 min flow of aqueous solution of EDC/NHS. Subsequently, the HBsAg in HEPES buffer (pH 7.5) was flowed over the surface. After the reaction, the surface is rinsed with the HEPES buffer and the surface mass density of the immobilized HBsAg can be estimated from the SPR wavelength shift before and after the immobilization. Fig. 4b reveals that the amount of antigen immobilized at the surface can be controlled by the reaction time with the HBsAg solution. The maximum surface coverage was obtained after approximately 10 min flow when the SPR response reached its plateau of $\Delta\lambda_{SPR} = 33.24$ nm.

3.3. Fouling of pristine and biofunctionalized poly(HPMA-co-CBMAA) brush

The antifouling properties of the poly(HPMA-*co*-CBMAA) brush were evaluated for human blood serum from healthy individuals. Since the immobilization of bioreceptors may induce impairment of the antifouling properties, the fouling from samples from individuals that showed negative response in the ELISA test was evaluated on brushes after the immobilization of HBsAg. No detectable shift in SPR wavelength $\Delta\lambda_{SPR}$ was observed from undiluted and 10% human blood serum samples as depicted in Figs. 5 and S4 in the SI. Therefore, the pristine poly(HPMA-*co*-CBMAA) provides resistance to the fouling similar to homopolymer brushes

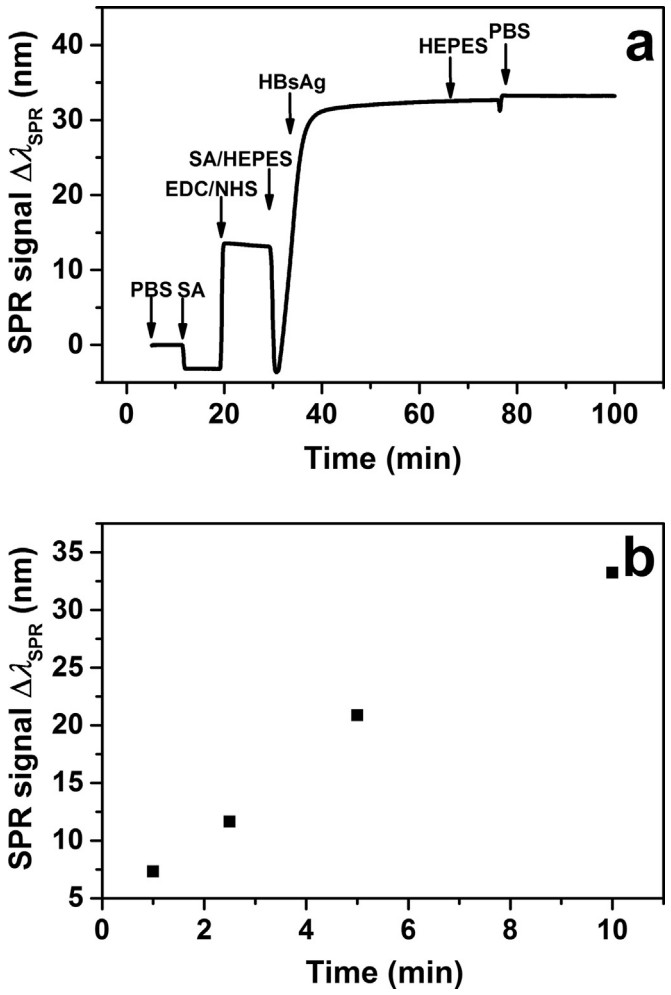

Fig. 4. (a) SPR measurement of the immobilization of HBsAg onto poly(HPMA-*co*-CBMAA) brush. The arrows indicate solutions changes (PBS – phosphate buffered saline buffer, pH 7.4; SA – sodium acetate buffer, pH 5; HEPES – HEPES buffer, pH 7.5; 0.2 M EDC and 0.05 M NHS; HBsAg 25 μg/mL in PBS). (b) Time-dependent immobilization of HBsAg onto poly(HPMA-*co*-CBMAA) brush.

of HPMA and CBMAA reported before (<0.3 ng cm^{-2}), the so far only brushes able to prevent the fouling from human blood, plasma and serum (de Los Santos Pereira et al., 2016; Kostina et al., 2012; Rodriguez-Emmenegger et al., 2011).

Importantly, the resistance to the fouling of poly(HPMA-*co*-CBMAA) is retained even after the post-modification with HBsAg (Fig. 5b). This is a key advancement as the post modification of brushes composed from individual homopolymers (HPMA and CBMAA) is known to severely deteriorate their antifouling properties (Vaisocherová et al., 2014). The negative effect on the homopolymer brushes may be ascribed to the reaction of too many functional groups (*e.g.*, carboxyl of CBMAA) leading to a net positive charge or crosslinking of the chains. The herein reported approach enables efficient biofunctionalization of the polymer brush due to the presence of carboxyl groups in CBMAA while preserving antifouling properties of the polymer brush owing to the HPMA units.

3.4. Detection of anti-HBs antibodies in clinical serum

We prepared a biosensing surface for the detection of antibodies against hepatitis B anti-HBs in clinical samples using SPR. The samples (A-H) were collected from 8 apparently healthy human donors. The total amount of sample needed for one analysis was only 15 μL. The diagnosis obtained by SPR were compared with the results obtained from ELISA, which was carried out by an independent certified laboratory on the same samples (SI Table S1). The tested group contained three negative samples (antibody titer below the detection limit of ELISA – 0.002 IU mL^{-1}), three positive (0.068–0.645 IU mL^{-1}) and two highly positive samples (>1 IU mL^{-1}).

Direct detection of anti-HBs in serum A-H was carried out using an SPR instrument and a sensor chip with poly(HPMA-*co*-CBMAA) brushes. For each assay, the SPR wavelength was tracked upon sequential flow of analyzed sample followed by the rinsing and reaction with secondary antibody (Fig. S5 in SI). For the direct detection format, the sensor response $\Delta\lambda_{SPR}$ was determined as the shift of SPR wavelength due to the binding of anti-HBs after 10 min flow of a sample followed by rinsing with a buffer. As seen in Fig. 6a, the direct assay allowed to clearly discriminate between positive and negative samples. The response of newly fabricated SPR biosensor shows a linear relationship with the concentration of *anti*-HBs obtained by ELISA (Fig. 6b). This response can be further amplified by the binding of a secondary anti-hIgG after the capture of anti-HBs. However, it must be noted that the linear function is not accurate as ELISA values in the high (>1 IU mL^{-1}) and low range (<0.002 IU mL^{-1}) is not able to differentiate between concentrations. For instance serum D, E, and H were below the detection limit of ELISA while our SPR was able to differentiate between these samples. Furthermore, serum A and C had values above 1 IU mL^{-1} and again the SPR could differentiate between them. The presented SPR sensor thus show excellent dynamic range superior to ELISA. The comparison of the SPR response to the binding of the target analyte and anti-hIgG shows similar SPR

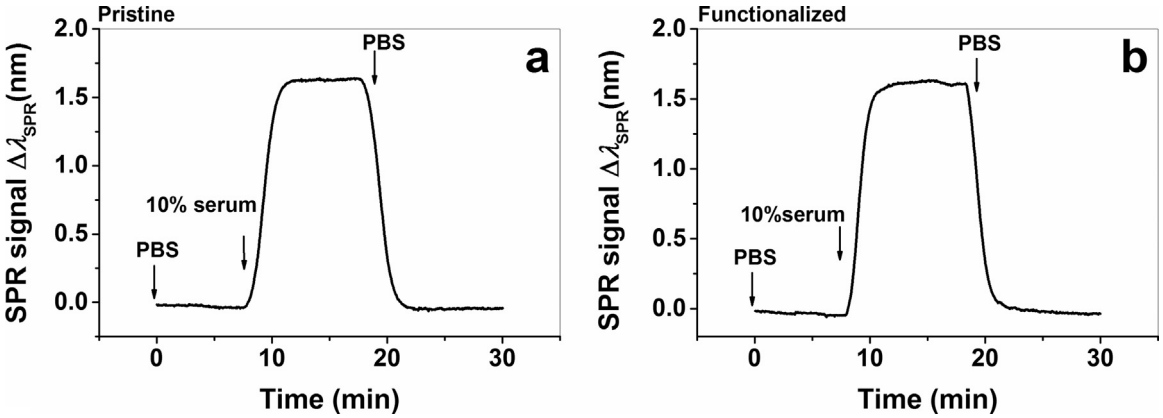

Fig. 5. SPR characterization of the fouling on pristine and functionalized poly(HPMA-*co*-CBMAA) brush: (a) pristine surface and (b) surface modified with HBsAg brought in contact with 10% serum.

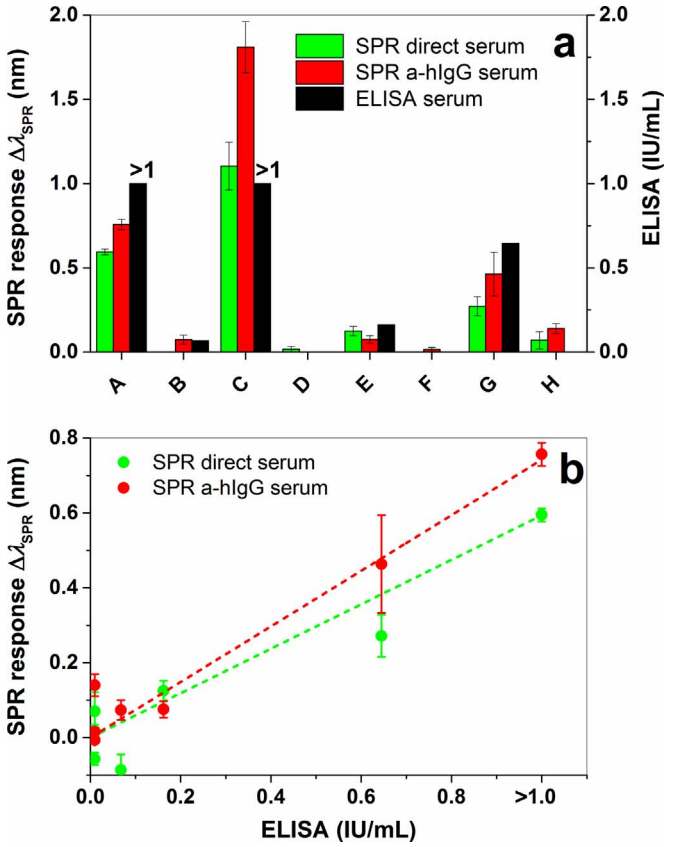

Fig. 6. (a) Analysis of anti-HBs antibodies in clinical serum samples from donors A-H by SPR in comparison to ELISA (green columns represent direct detection of anti-HBs; red columns represent secondary response; black columns represent ELISA results). (b) SPR sensor response to clinical serum samples is plotted as a function of concentration in serum determined ELISA. Lines represent linear fits (R=0.9 and 0.96). (For interpretation of the references to color in this figure legend, the reader is referred to the web version of this article.)

response. Thus, roughly each captured anti-HBs was captured by one anti-hIgG. This observation suggests that steric hindrance is not significant. Moreover, the assay is based on antigen-antibody interaction that can be easily disrupted by changing pH or ionic strength of the buffer. To demonstrate this we treated the biosensor with 20 mM glycine-HCl buffer (pH 1.5) after detection. It was possible to regenerate about 95% of the capacity of the sensor after 3 cycles of measurement-regeneration (Fig. S6 in SI).

It is worth of noting that previous works on SPR detection of HBV and antibodies against HBsAg have been almost solely carried out in model samples spiked with the analyte in either buffer or highly diluted serum at concentrations orders of magnitude higher than the biologically relevant (Choi et al., 2014; Chuang et al., 2012, 2005; Hwang et al., 2005; Uzun et al., 2009; Wang et al., 2010; Zheng et al., 2010). Moreover, in those studies carried out in dilute serum, the signal needed to be compensated by a reference to subtract the response due to the unspecific adsorption of serum. While that approach can be applied in model experiments with pooled serum samples, the large difference in fouling from different donors makes this means of fouling compensation not feasible for real clinical samples (Pereira et al., 2014). The results presented herein show that by suppressing the fouling below the limit of detection of the SPR, it was possible to quantify antibodies against HBsAg in clinical serum samples.

4. Conclusions

Using a novel biointerface architecture we report the detection of anti-HBs in real (non-spiked) clinical serum samples. The interface is based on poly(HPMA-*co*-CBMAA) brushes functionalized with bioreceptors. The new poly(HPMA-*co*-CBMAA) brushes were thoroughly characterized and demonstrated to exhibit antifouling properties as well as high binding capacity. Remarkably, these brushes remained non-fouling even after the biofunctionalization with the hepatitis B surface antigen. The combination of unmatched resistance to fouling, low sample consumption (15 μL), and fast label-free SPR detection (10 min) with accuracy comparable to established ELISA is envisioned to set the way to new biosensor technologies that can be deployed outside centralized laboratories.

Acknowledgment

This work was supported by the Grant Agency of the Czech Republic (GACR) under Contract no. 15-09368Y and P205-12-G118, the Ministry of Education, Youth and Sports of CR within the National Sustainability Program II (Project BIOCEV-FAR LQ1604), by the project "BIOCEV" (CZ.1.05/1.1.00/02.0109) and by OPPK (CZ.2.16/3.1.00/21545), from the European Regional Development Fund. In addition, this work was partially supported by Austrian Science Fund (FWF) through the project ACTIPLAS (P 244920-N20), and FEMTECH – Frauen in Forschung und Technologie Initiative of the Austrian Ministry for Transportation, Innovation and Technology.

Appendix A. Supplementary material

Supplementary data associated with this article can be found in the online version at http://dx.doi.org/10.1016/j.bios.2016.05.014.

References

Blaszykowski, C., Sheikh, S., Thompson, M., 2012. Surface chemistry to minimize fouling from blood-based fluids. Chem. Soc. Rev. 41 (17), 5599–5612.
Blaszykowski, C., Sheikh, S., Thompson, M., 2015. A survey of state-of-the-art surface chemistries to minimize fouling from human and animal biofluids. Biomater. Sci. 3 (10), 1335–1370.
Brault, N.D., et al., 2013. Directly functionalizable surface platform for protein arrays in undiluted human blood plasma. Anal. Chem. 85 (3), 1447–1453.
Cho, W.K., Kang, S.M., Lee, J.K., 2014. Non-biofouling polymeric thin films on solid substrates. J. Nanosci. Nanotechnol. 14 (2), 1231–1252.
Choi, Y.-H., et al., 2014. Development of SPR biosensor for the detection of human hepatitis B virus using plasma-treated parylene-N film. Biosens. Bioelectron. 56, 286–294.
Chuang, T.-L., Wei, S.-C., Lee, S.-Y., Lin, C.-W., 2012. A polycarbonate based surface plasmon resonance sensing cartridge for high sensitivity HBV loop-mediated isothermal amplification. Biosens. Bioelectron. 32 (1), 89–95.
Chung, J.W., Kim, S.D., Bernhardt, R., Pyun, J.C., 2005. Application of SPR biosensor for medical diagnostics of human hepatitis B virus (hHBV). Sens. Actuator B – Chem. 111–112, 416–422.
de los Santos Pereira, A., Riedel, T., Brynda, E., Rodriguez-Emmenegger, C., 2014. Hierarchical antifouling brushes for biosensing applications. Sens. Actuator B – Chem. 202, 1313–1321.
de Los Santos Pereira, A., et al., 2016. Antifouling polymer brushes displaying antithrombogenic surface properties. Biomacromolecules 17 (3), 1179–1185.
Gitlin, N., 1997. Hepatitis B: diagnosis, prevention, and treatment. Clin. Chem. 43 (8), 1500–1506.
Harbarth, S., Szucs, T., Berger, K., Jilg, W., 2000. The economic burden of Hepatitis B in Germany. Eur. J. Epidemiol. 16 (2), 173–177.
Herrwerth, S., Eck, W., Reinhardt, S., Grunze, M., 2003. Factors that determine the protein resistance of oligoether self-assembled monolayers – internal hydrophilicity, terminal hydrophilicity, and lateral packing density. J. Am. Chem. Soc. 125 (31), 9359–9366.
Hollinger, F.B., Liang, T.J., 2001. Hepatitis B virus. Fields Virol. 4, 2971–3036.
Homola, J., 2008. Surface plasmon resonance sensors for detection of chemical and biological species. Chem. Rev. 108, 462–493.
Homola, J., et al., 2002. Spectral surface plasmon resonance biosensor for detection of staphylococcal enterotoxin B in milk. Int. J. Food Microbiol. 75 (1–2), 61–69.
Hwang, S.Y., et al., 2005. Quantitative assay of hepatitis B surface antigen by using

surface plasmon resonance biosensor. Biotechnol. Bioprocess Eng. 10 (4), 309–314.
Jiang, S., Cao, Z., 2010. Ultralow-fouling, functionalizable, and hydrolyzable zwitterionic materials and their derivatives for biological applications. Adv. Mater. 22 (9), 920–932.
Kostina, N.Y., et al., 2012. Non-fouling hydrogels of 2-hydroxyethyl methacrylate and zwitterionic carboxybetaine (Meth)acrylamides. Biomacromolecules 13 (12), 4164–4170.
Lesmana, L.A., et al., 2006. Hepatitis B: overview of the burden of disease in the Asia-Pacific region. Liver Int. 26 (Suppl 2), 3–10.
Lozano, R., et al., 2012. Global and regional mortality from 235 causes of death for 20 age groups in 1990 and 2010: a systematic analysis for the Global Burden of Disease Study 2010. Lancet 380 (9859), 2095–2128.
Lu, X., et al., 2013. A gold nanorods-based fluorescent biosensor for the detection of hepatitis B virus DNA based on fluorescence resonance energy transfer. Analyst 138 (2), 642–650.
Mahmud, G., et al., 2011. Carboxybetaine methacrylate polymers offer robust, long-term protection against cell adhesion. Langmuir 27 (17), 10800–10804.
Pereira, A.d.l.S., et al., 2014. Use of pooled blood plasmas in the assessment of fouling resistance. RSC Adv. 4 (5), 2318–2321.
Poorolajal, J., et al., 2010. Long-term protection provided by hepatitis B vaccine and need for booster dose: a meta-analysis. Vaccine 28 (3), 623–631.
Pop-Georgievski, O., et al., 2013. Biomimetic non-fouling surfaces: extending the concepts. J. Mater. Chem. B 1 (22), 2859–2867.
Riedel, T., Majek, P., Rodriguez-Emmenegger, C., Brynda, E., 2014. Surface plasmon resonance: advances of label-free approaches in the analysis of biological samples. Bioanalysis 6 (24), 3325–3336.
Riedel, T., et al., 2013. Complete identification of proteins responsible for human blood plasma fouling on poly(ethylene glycol)-based surfaces. Langmuir 29 (10), 3388–3397.
Rodriguez-Emmenegger, C., et al., 2011. Polymer brushes showing non-fouling in blood plasma challenge the currently accepted design of protein resistant surfaces. Macromol. Rapid Commun. 32 (13), 952–957.
Rodriguez-Emmenegger, C., et al., 2012a. Controlled/living surface-initiated ATRP of antifouling polymer brushes from gold in PBS and blood sera as a model study for polymer modifications in complex biological media. Macromol. Biosci. 12 (4), 525–532.
Rodriguez-Emmenegger, C., Houska, M., Alles, A.B., Brynda, E., 2012b. Surfaces resistant to fouling from biological fluids: towards bioactive surfaces for real applications. Macromol. Biosci. 12 (10), 1413–1422.
Rodriguez-Emmenegger, C., et al., 2015. Quantifying bacterial adhesion on antifouling polymer brushes via single-cell force spectroscopy. Polym. Chem. 6 (31), 5740–5751.
Rodriguez-Emmenegger, C., et al., 2013. Controlled cell adhesion on poly(dopamine) interfaces photopatterned with non-fouling brushes. Adv. Mater. 25 (42), 6123–6127.
Rodriguez Emmenegger, C., et al., 2009. Interaction of blood plasma with antifouling surfaces. Langmuir 25 (11), 6328–6333.
Shi, X., et al., 2012. Cell adhesion on a POEGMA-modified topographical surface. Langmuir 28 (49), 17011–17018.
Stewart, M.E., et al., 2008. Nanostructured plasmonic sensors. Chem. Rev. 108 (2), 494–521.
Surman, F., et al., 2015. Polymer brushes interfacing blood as a route toward high performance blood contacting devices. Macromol. Biosci. 15 (5), 636–646.
Tighe, P.J., Ryder, R.R., Todd, I., Fairclough, L.C., 2015. ELISA in the multiplex era: potentials and pitfalls. Proteom. Clin. Appl. 9 (3–4), 406–422.
Uzun, L., Say, R., Unal, S., Denizli, A., 2009. Production of surface plasmon resonance based assay kit for hepatitis diagnosis. Biosens. Bioelectron. 24 (9), 2878–2884.
Vaisocherová, H., et al., 2014. Functionalized ultra-low fouling carboxy- and hydroxy-functional surface platforms: functionalization capacity, biorecognition capability and resistance to fouling from undiluted biological media. Biosens. Bioelectron. 51, 150–157.
Vaisocherová, H., et al., 2008. Ultralow fouling and functionalizable surface chemistry based on a zwitterionic polymer enabling sensitive and specific protein detection in undiluted blood plasma. Anal. Chem. 80 (20), 7894–7901.
Wang, X., et al., 2010. Gold nanorod-based localized surface plasmon resonance biosensor for sensitive detection of hepatitis B virus in buffer, blood serum and plasma. Biosens. Bioelectron. 26 (2), 404–410.
Yang, W., et al., 2009. Pursuing “zero” protein adsorption of poly(carboxybetaine) from undiluted blood serum and plasma. Langmuir 25 (19), 11911–11916.
Yao, C.-Y., Fu, W.-L., 2014. Biosensors for hepatitis B virus detection. World J. Gastroenterol. 20 (35), 12485–12492.
Zheng, S., et al., 2010. Label-free optical diagnosis of hepatitis B virus with genetically engineered fusion proteins. Talanta 82 (2), 803–809.